

1 **Freshwater dispersion stability of PAA-stabilised cerium oxide nanoparticles and**
2 **toxicity towards *Pseudokirchneriella subcapitata***

3
4 Andy Booth*¹, Trond Størseth¹, Dag Altin², Andrea Fornara³, Anwar Ahniyaz³, Harald
5 Jungnickel⁴, Peter Laux⁴, Andreas Luch⁴, Lisbet Sørensen¹

6
7 ¹SINTEF Materials and Chemistry, Trondheim N-7465, Norway

8 ²BioTrix, Trondheim N-7022, Norway

9 ³German Federal Institute for Risk Assessment (BfR), Department of Product Safety, Berlin,
10 Germany

11 ⁴SP Chemistry, Materials and Surfaces, Drottning Kristinas vag 45, SE-11686, Stockholm,
12 Sweden

13
14
15
16 *Corresponding author: andy.booth@sintef.no, +47 93089510

19 **Abstract**

20 An aqueous dispersion of poly (acrylic acid)-stabilised cerium oxide (CeO₂) nanoparticles
21 (PAA-CeO₂) was evaluated for its stability in a range of freshwater ecotoxicity media
22 (MHRW, TG 201 and M7), with and without natural organic matter (NOM). In a 15 day
23 dispersion stability study, PAA-CeO₂ did not undergo significant aggregation in any media
24 type. Zeta potential varied between media types and was influenced by PAA-CeO₂
25 concentration, but remained constant over 15 days. NOM had no influence on PAA-CeO₂
26 aggregation or zeta potential. The ecotoxicity of the PAA-CeO₂ dispersion was investigated in
27 72 h algal growth inhibition tests using the freshwater microalgae *Pseudokirchneriella*
28 *subcapitata*. PAA-CeO₂ EC₅₀ values for growth inhibition (GI; 0.024 mg/L) were 2-3 orders
29 of magnitude lower than pristine CeO₂ EC₅₀ values reported in the literature. The
30 concentration of dissolved cerium (Ce³⁺/Ce⁴⁺) in PAA-CeO₂ exposure suspensions was very
31 low, ranging between 0.5-5.6 µg/L. Free PAA concentration in the exposure solutions
32 (0.0096-0.0384 mg/L) was significantly lower than the EC₁₀ growth inhibition (47.7 mg/L)
33 value of pure PAA, indicating free PAA did not contribute to the observed toxicity. Elemental
34 analysis indicated up to 38% of the total Cerium becomes directly associated with the algal
35 cells during the 72 h exposure. TOF-SIMS analysis of algal cell wall compounds indicated
36 three different modes of action, including a significant oxidative stress response to PAA-CeO₂
37 exposure. In contrast to pristine CeO₂ nanoparticles, which rapidly aggregate in standard
38 ecotoxicity media, PAA-stabilised CeO₂ nanoparticles remain dispersed and available to
39 water column species. Interaction of PAA with cell wall components, which could be
40 responsible for the observed biomarker alterations, could not be excluded. This study
41 indicates that the increased dispersion stability of PAA-CeO₂ leads to an increase in toxicity
42 compared to pristine non-stabilised forms.

43

44 **Keywords** – nanoparticles; CeO₂; dispersion stability; ecotoxicity; freshwater algae

45

46 **1. Introduction**

47 Owing to their radical scavenging and UV-filtering properties, cerium oxide (CeO₂)
48 engineered nanoparticles (ENPs) offer a solution to several technological challenges.
49 Currently, major uses include CeO₂ ENP-based catalytic filters to reduce exhaust particle
50 emissions from diesel combustion (Park et al., 2007) and as an antioxidant, protecting
51 biological tissue from oxidative stress induced by reactive oxygen species (ROS) (Karakoti et
52 al., 2008). Other engineering and biological applications of CeO₂ ENPs include solid-oxide
53 fuel cells, high-temperature oxidation protection materials, catalytic materials, solar cells and
54 potential pharmacological agents in bioanalysis, biomedicine, drug delivery, and
55 bioscaffolding (Xu et al., 2014) (and references therein).

56

57 Inevitably, CeO₂ ENPs will be released to the aquatic environment, where their fate and
58 potential impacts will depend on their physicochemical properties (size, shape, surface
59 chemistry) and environmental conditions (pH, ionic strength, colloids and natural organic
60 matter (NOM) content) (van Hoecke et al., 2011; Booth et al., 2013). In aqueous
61 environments, CeO₂ ENPs may undergo a variety of transformation processes, including
62 homo-aggregation, settling and dissolution. Interaction with other particulates (hetero-
63 aggregation) or compounds present in the water column may drive the aggregation process or
64 help stabilise dispersed ENPs. Aggregation and sorption behaviour can have a significant
65 effect on ENP toxicity (Adegboyega et al., 2012; Baalousha et al., 2013; Louie et al., 2013).

66

67 A study investigating the behaviour of CeO₂ ENPs in different natural waters showed that
68 sedimentation and hetero-aggregation with natural colloids were the main removal
69 mechanisms (Quik et al., 2012). The concentration and composition of NOM in natural waters
70 varies significantly (Wang et al., 2011) and influences ENP behaviour (Keller et al., 2010;

71 Quik et al., 2010; Quik et al., 2012; Loosli et al., 2013; Gallego-Urrea et al., 2014). Fulvic and
72 humic acids present in NOM can stabilise CeO₂ ENPs in natural waters and in algae growth
73 media, either by electrostatic or steric repulsion (Quik et al., 2010). Furthermore, pH
74 significantly affects NOM adsorption to CeO₂ ENPs, thus influencing CeO₂ ENP aggregate
75 size (van Hoecke et al., 2011). In freshwater and under conditions relevant for
76 ecotoxicological tests CeO₂ ENPs tend to agglomerate, which can have effects on
77 bioavailability and toxicity (Rodea-Palomares et al., 2011; Röhder et al., 2014).

78
79 The ecotoxicity of a wide range of unmodified ('pristine') CeO₂ ENPs to aquatic species such
80 as bacteria, algae, zooplankton and fish, has been the subject of many studies (van Hoecke et
81 al., 2009; Johnston et al., 2010; García et al., 2011; Sánchez et al., 2011; Manier et al., 2013;
82 Röhder et al., 2014). However, there still remains limited information on the effects of CeO₂
83 ENPs to algae. Growth inhibition of the freshwater microalga *Pseudokirchneriella*
84 *subcapitata* has been reported in different studies over a concentration range of 4.4–29.6 mg
85 L⁻¹ CeO₂ ENPs (van Hoecke et al., 2009; Rogers et al., 2010; Manier et al., 2011; Rodea-
86 Palomares et al., 2011; Manier et al., 2013). The measured dissolved cerium(III)
87 concentration in CeO₂ ENPs suspensions was low and therefore not considered to be relevant
88 for toxicity of CeO₂ ENPs (van Hoecke et al., 2009; Rogers et al., 2010; Rodea-Palomares et
89 al., 2011). In most studies CeO₂ ENPs did not form stable dispersions in algal exposure
90 media, undergoing different degrees of agglomeration (Rodea-Palomares et al., 2011).
91 However, primary particle size was found to influence toxicity irrespective of agglomeration,
92 with smaller nominal diameters increasing growth inhibition (van Hoecke et al., 2009).

93
94 Importantly, CeO₂ ENP growth inhibition in algae appears to be significantly influenced by
95 the dispersion method and age of the suspension (Manier et al., 2011; Manier et al., 2013). In

96 all studies, flocculation of algae cells or clustering of CeO₂ ENPs around the cell surface was
97 observed. Direct contact of CeO₂ ENPs with algae can cause membrane damage in *P.*
98 *subcapitata* and may be responsible for the observed toxicity (Rogers et al., 2010; Rodea-
99 Palomares et al., 2011). Under experimental light conditions, CeO₂ ENPs can generate
100 hydroxyl radicals causing lipid peroxidation (Rogers et al., 2010), whilst an increase in
101 intracellular reactive oxygen species (ROS) in algae has been observed (Rodea-Palomares et
102 al., 2012).

103
104 Increasingly, ENP physicochemical properties are being modified in order to improve their
105 performance in different technologies and applications. Stabilising agents to maintain ENPs in
106 aqueous dispersion are becoming common, resulting in the surface of the ENPs being coated
107 by organic compounds (Sehgal et al., 2005; Salazar-Sandoval et al., 2014). There is a need to
108 understand how these modified ENPs behave in the environment and what impacts such
109 modifications have on their toxicity, especially compared to the large body of data available
110 for pristine ENPs. Garcia et al. (García et al., 2011) performed a range of standardised aquatic
111 ecotoxicity tests on CeO₂ ENP dispersions stabilised with hexamethylenetetramine (HMT).
112 The CeO₂ ENPs exhibited high toxicity to *D. magna* (48 h acute LC₅₀ was 0.012 mg/mL) and
113 *V. fischeri* (Microtox® bioluminescence inhibition was >80 % at 0.064 mg/mL). The HMT
114 stabiliser was demonstrated not to be toxic in this study, but may play a role in the observed
115 toxicity of the CeO₂ ENPs.

116
117 In the current study, the dispersion stability of poly (acrylic acid)-stabilised CeO₂ ENPs
118 (PAA-CeO₂) in a range of common ecotoxicity media and their subsequent ecotoxicity to *P.*
119 *subcapitata* was assessed. The stability and aggregation of PAA-CeO₂ was studied over time
120 and the influence of Suwannee River NOM (SR-NOM) on dispersion stability was also

121 investigated. Ecotoxicity of the PAA-CeO₂ and pure PAA to *P. subcapitata* was assessed
122 using a modified version of the algal growth inhibition method (OECD 201) to overcome the
123 problem of algal cell ‘shading’ by ENPs when measuring algal growth by fluorescence.
124 Changes in the levels of algal cell wall compounds were monitored using TOF-SIMS.
125 Particulate CeO₂ and dissolved Ce³⁺/Ce⁴⁺ concentration was determined by ultracentrifugation
126 and HR-ICP-MS analysis. The total Ce (dissolved plus particulate) concentration in selected
127 filtered (no algae present) and non-filtered (algae present) exposure samples was determined
128 using HR-ICP-MS to investigate PAA-CeO₂ uptake/adsorption by the algae.

129

130 **2. Experimental**

131 *2.1. Chemicals and materials*

132 All chemicals were of analytical grade, and deionised water was from a Miele Aqua
133 Purificator C7749 system. Poly acrylic acid (PAA, average MW<1800) was purchased from
134 Sigma Aldrich. Suwannee River NOM (SR-NOM) was purchased from International Humic
135 Substances Society (St. Paul, USA). Medium hard synthetic water (MHRW) was made as
136 according to US EPA 821-R-02-12 (US EPA, 2002), media for freshwater algae (TG 201)
137 was made according to OECD Guideline 201, media for *Daphnia magna* (M7) was made
138 according to OECD Guideline 202. All salts and compounds used in the preparation of media
139 water were of analytical grade and supplied by acknowledged international manufacturers.
140 Finally, the pH of the solutions was adjusted as according to the guidelines.

141

142 *2.2. CeO₂ nanoparticle synthesis and characterisation*

143 CeO₂ nanoparticles were synthesised by thermolysis of Ce(NO₃)₄ at high temperature,
144 resulting in homogenous precipitation of a cerium oxide nanoparticle pulp (Chane-Ching,
145 1994). To stabilise the CeO₂ nanoparticles in water, PAA was employed as an anionic

146 stabiliser and added in excess (Sehgal et al., 2005). A final PAA-stabilised colloidal
147 dispersion of CeO₂ particles (PAA-CeO₂) in MilliQ water (10% wt., 100 mg/L), with a pH of
148 8.5, was prepared for further study. Relevant physical and chemical characterisation
149 techniques were employed to study the PAA-CeO₂. The zeta potential and average
150 hydrodynamic radius (by volume; dynamic light scattering, DLS) of the stock solution was
151 determined using a Malvern Zetasizer. A Phillips CM30 and a Jeol 2100 Transmission
152 electron microscopes (TEM) operated at 150kV and 120kV respectively, both equipped with a
153 LaB6 electron filament were used to investigate individual PAA-CeO₂ crystallite size and
154 shape. Samples were prepared by adding a droplet of the PAA-CeO₂ stock solution to a holey
155 copper grid and allowing the water to evaporate. The Jeol 2100 was equipped with an INCA
156 (from Oxford Instruments) Energy-dispersive X-ray spectroscope (EDX) which was used to
157 study the elemental composition of the PAA-CeO₂ stock material and identify any significant
158 impurities. For the same purpose, Selected Area Electron Diffraction (SAED) pattern analysis
159 was performed with the CM30.

160

161 *2.3. PAA analysis*

162 The concentration of free/excess PAA in the PAA-CeO₂ stock solution, and any subsequent
163 dilutions, required determination in order to account for any ecotoxicological effect. As the
164 PAA was a complex mixture of poly acrylic acid molecules with an average molecular weight
165 of 1800, an NMR-based analysis and quantification method was used. A pure PAA standard
166 in deionised water was prepared and serially diluted to create a calibration curve (0.01 - 10
167 mg/L). To determine the free PAA concentration in the PAA-CeO₂ stock solution, a sample
168 was diluted in deionised water to a PAA-CeO₂ concentration of 10 mg/L. A 5 mL aliquot was
169 then subjected to ultracentrifugation at 65,000 rpm for 60 min (Sorvall WX Ultra, rotor T-
170 865). The supernatant was collected and analysed to quantify the amount of dissolved PAA

171 remaining. NMR sample preparation was done by adding 20 μ l of D₂O containing 1mM 3-
172 (Trimethylsilyl)propionic-2,2,3,3-d₄ acid sodium salt (TSP) to 180 μ l of standard solutions
173 and supernatant from sample centrifugation. ¹H-NMR spectra were recorded using a Bruker
174 DRU 600 spectrometer (Bruker BioSpin GMBH, Rheinstetten, Germany) operating at 600.13
175 MHz for ¹H using a 1D NOESY (noesygppr1d) pulse sequence from the Bruker pulse
176 sequence library for suppression of residual water. The region from 3.2-0.5ppm was used for
177 the PAA and this was calibrated against the TSP peak. The PAA concentration of the
178 centrifuged sample was determined by the linear regression equation of the standard curve.

179

180

181 *2.4. Particulate CeO₂ and dissolved Ce³⁺/Ce⁴⁺ analysis*

182 In order to determine the dissolved Ce³⁺/Ce⁴⁺ concentration present in the stock solution, a 10
183 mg/L dilution was prepared and subjected to ultracentrifugation as described above. The
184 supernatant (0.2 mL) was collected and transferred to an ultra-inert sample tube prior to
185 analysis by high resolution inductively coupled plasma mass spectrometry (HR-ICP-MS;
186 Element 2, Thermoelectric) to determine the Ce³⁺/Ce⁴⁺ concentration. Samples were analysed
187 without any pre-treatment except dilution in 0.1 M nitric acid.

188

189 *2.5. Dispersion stability studies*

190 Moderately hard reconstituted water (MHRW) (US EPA, 2002), TG 201 media (freshwater
191 algae, OECD) (OECD, 2011) and M7 (*Daphnia magna*, OECD) were prepared according to
192 the relevant guidelines using reagent grade chemicals and deionised water. For the
193 experiments investigating the influence of natural organic matter (NOM) on dispersion
194 stability, SR-NOM was dissolved in the media at an initial concentration of 20 mg/L and
195 stirred overnight using a magnetic stirrer. After 1 day of stirring, the media-NOM solutions

196 were filtered using a Nalgene® filtration unit (0.22 μm pore size) to remove any non-
197 dissolved particulate matter. The total organic carbon (TOC) in the resulting solution was
198 determined as 8-9 mg/L (Sievers 900 Portable Turbo instrument). The specific conductivity of
199 each dispersion media was determined, where $M7 = 679.7 \mu\text{S cm}^{-1}$, $M7\text{-NOM} = 666.33 \mu\text{S}$
200 cm^{-1} , $MHRW = 312.7 \mu\text{S cm}^{-1}$, $MHRW\text{-NOM} = 308.2 \mu\text{S cm}^{-1}$, $TG201 = 163.6 \mu\text{S cm}^{-1}$, and
201 $TG201\text{-NOM} = 163.4 \mu\text{S cm}^{-1}$.

202

203 The stock dispersion of PAA-CeO₂ was sonicated immediately prior to sub-sampling to
204 ensure homogeneity of the sample prior to dilution in the different media solutions. Two
205 different nominal start concentrations were included in the study; 1 and 0.01 mg/L – three
206 parallels of each concentration in every media. Immediately prior to the first sampling, the
207 samples were homogenised by sonicating for 10 minutes. After this, the samples were left still
208 for the duration of the experiment. Each sample tube was sampled for particle number
209 measurement (dynamic light scattering, DLS) and surface charge measurement (zeta
210 potential) at day 0, 2, 5, 7, 12 and 15.

211

212 *2.6. Average particle size and zeta potential measurements*

213 The hydrodynamic particle size distribution and zeta potential of the PAA-CeO₂ suspensions
214 was measured using a Zetasizer Nanorange ZS instrument (Malvern, UK). For the size
215 measurements, a small volume of the sample (~0.5 mL) was diluted with the appropriate
216 media solution in a disposable polystyrene cuvette (2.5 mL). The laser source was 632.8 nm
217 with 173 ° backscatter. The zeta potential was measured on the same solution after transfer to
218 a capillary zeta cell. The measurements were performed with automatically optimised number
219 of runs (10-30).

220

221 2.7. *Algae ecotoxicity studies*

222 The ecotoxicity of PAA-CeO₂, as well as the toxicity of the pure PAA, was investigated using
223 the freshwater algae *Pseudokirchneriella subcapitata* (clone NIVA-CHL1) in a 72 h static
224 growth inhibition test according to OECD 201 (OECD, 2011). For both test materials, a 72 h
225 range-finding pre-test was conducted with sampling at Day 0 and Day 3 and a tentative EC₅₀
226 value determined. Based on these results, 72 h full tests with sampling at Day 0, 1, 2 and 3
227 was completed (Day 0 samples were collected immediately after preparation to provide
228 baseline values). The pure PAA stabiliser was tested in 12 mL plastic tubes (sample volume
229 10 mL), at concentrations of 30, 60, 100, 200, 300, 400, 600, 800, 1000 mg/L. As the
230 exposure solutions were free of particulate material, except for the algal cells, *in vivo*
231 fluorescence from chlorophyll was measured directly on the exposure solutions by inserting
232 the tubes in a Spectrophotometer.

233

234 Due to the nature of the tested substances, the standard OECD 201 protocol was modified for
235 the PAA-CeO₂. Exposures were completed in 250 ml Erlenmeyer flasks covered with a
236 beaker during incubation at nominal concentrations of 15 (5.5), 25 (12.6), 40 (16.8), 60
237 (25.4), 100 (32.7) and 200 (67.5) µg/L; actual concentrations determined by HR-ICP-MS
238 given in parentheses (Table 1). In order to overcome potential issues with shading of the algal
239 cells during quantification of the growth, the standard fluorescence method was replaced with
240 a modified version of the ISO method ‘Measurement of biochemical Parameters -
241 Spectrometric determination of the chlorophyll-a concentration (ISO 10260: 1992)’. After
242 completion of the exposure period (72 h) the exposure media (10 mL) was filtered using a 0.7
243 µm glass fibre filter (Whatman GF/F), and the aqueous phase discarded. The filter was then
244 allowed to dry before being added to a vial containing hot ethanol at 75 °C (10 mL) and the
245 chlorophyll pigments extracted by shaking for 5 min. Once cooled to room temperature, the

246 sample was filtered again to remove any particulate material and the eluent was transferred to
247 a 4.5 mL cuvette and analysed using fluorometer (Turner TD-700, Turner Designs, US). At
248 Day 0 and Day 3, 2 mL aliquots of the exposure solution (before and after the algal filtration
249 step) were collected and subjected to analysis by HR-ICP-MS to quantify the CeO₂
250 concentration.

251

252 *2.8. Biokinetics*

253 The metabolic changes of the cell wall after PAA-CeO₂ exposure algal cells were investigated
254 using TOF-SIMS. 10 µL of the algal exposure solution was pipetted onto a gold wafer, fast
255 frozen in liquid nitrogen and stored at -80°C until the TOF-SIMS analysis was performed. Ion
256 spectra measurements were performed using a TOF-SIMS V instrument (IONTOF GmbH,
257 Münster, Germany) with a 30 keV nano-bismuth primary ion beam source. The ion currents
258 were measured to be 0.5 pA at 5 kHz using a Faraday cup. A pulse of 0.7 ns from the
259 bunching system resulted in a mass resolution that usually exceeded 5000 (full width at half-
260 maximum) at m/z <500 in negative mode. The primary ion dose was controlled below 10¹²
261 ions cm⁻² to ensure static SIMS conditions (Thompson et al., 2004; Jungnickel et al., 2005;
262 Haase et al., 2011; Tentschert et al., 2013).

263

264 *2.9. Statistical analyses and calculations*

265 Algal growth rates were calculated by linear regression in Excel v.14.3.9 for Mac OS X
266 (Microsoft Corp., USA) based on the daily increase in biomass measured as fluorescence.
267 Increase in algal biomass during exposure was calculated in Excel as the integral under the
268 growth curve (OECD, 2002). Prior to calculation of effect concentrations the calculated
269 values were normalised to control performance by calculating the percent inhibition. The
270 software GraphPad Prism v5.0b for Mac OS X (GraphPad Software, San Diego, USA) was

271 used for calculation of effect concentrations (EC_x) and data plotting in the ecotoxicity
272 bioassays. EC_{50} -values were calculated by performing a non-linear regression with a variable
273 slope on the calculated inhibition in growth rates and biomass production at the end of
274 exposure. Constraints were placed at 0 and 100% effect forcing the effect concentrations to be
275 calculated within this span thus eliminating the effect of any stimulation in growth. Values for
276 EC_{10} were calculated in a similar way by using the log(agonist) vs. response (Find
277 ECanything) function in GraphPad Prism on the same data set with the same constrains, and
278 applying least squares fit, as when calculating the EC_{50} -values.

279
280 Statistical analysis of the ToF-SIMS data was performed as described in detail elsewhere
281 (Thompson et al., 2004; Jungnickel et al., 2005; Haase et al., 2011; Tentschert et al., 2013). In
282 brief, the acquired data were binned to 1u. Data processing was carried out with the statistical
283 package SPSS+ (version 12.0.2G) using the mass range between 200 and 1700 mass units to
284 detect significant differences between treated cells at time point 0 and treated cells at time
285 point 3 days. Ions lower than mass 200 were excluded from the study to avoid contaminating
286 ions from salts, system contaminants, and other medium components. Each acquired spectrum
287 was then normalised, setting the peak sum to 100%. A Principal Component Analysis (PCA)
288 was performed using all ions. To show that data sets could be separated with a supervised
289 model from each other a Fisher's discriminant analysis was performed. The performance of
290 the discriminant model was verified by applying the cross-validation procedure based on the
291 "leave-one-out" cross-validation formalism.

292

293

294 **3. Results and discussion**

295 *3.1. CeO₂ nanoparticle synthesis and characterisation*

296 Key physicochemical parameters of the PAA-CeO₂ stock solution are presented in Table S1
297 in Supplementary Information. The zeta potential of the PAA-CeO₂ stock solution was
298 determined as -25mV, indicating moderate stability of the particles. The average
299 hydrodynamic radius of the PAA-CeO₂ stock solution (determined by volume using DLS)
300 was determined as 84 nm, with a poly dispersity index of 0.234. The crystallite size of the
301 individual CeO₂ particles was determined using TEM as between 4-10 nm, and generally
302 spherical in shape (Figure S1, Supplementary Information). These results indicate that some
303 degree of aggregation or agglomeration of the PAA-CeO₂ particles had occurred leading to
304 the higher hydrodynamic radius determined by DLS. EDX and SAED analysis was used to
305 investigate the purity of the PAA-CeO₂ stock material (Figure S2, Supplementary
306 Information). EDX analysis of the stock PAA-CeO₂ indicated trace amounts of Au, Co, Na
307 and Cl atoms. SAED pattern analysis confirmed that most of the material consists of CeO₂
308 nanoparticles (CeO₂ has a cubic unit cell, space group Fm-3m (225) and a = 5.412 Å).

309

310 3.2. PAA Analysis

311 The concentration of pure PAA in the 10 mg/L PAA-CeO₂ stock solution was 6.39 mg/L,
312 which represented (63.9% of the CeO₂ concentration). The concentration of pure PAA in the
313 algae exposure solutions ranged from 0.0096-0.128 mg/L (Table 1).

314

315 3.3. Dispersion stability studies

316 The PAA-CeO₂ did not undergo significant aggregation over 15 d in any media type (Figure 1
317 A-C). After 15 d, the 0.01 mg/L PAA-CeO₂ dispersions do appear to exhibit larger average
318 hydrodynamic sizes than 1.0 mg/L dispersions, however this could be an artefact of the DLS
319 approach which can be sensitive to differences in analyte concentration. It has been suggested
320 that intensity averaged hydrodynamic sizes from DLS analysis, whilst more frequently

321 reported, often are significantly higher than number averaged sizes (Gallego-Urrea et al.,
322 2014). Furthermore, the backscatter angle of 173° also promotes the size distribution towards
323 lower particle sizes through increased elimination of scattering from larger particles. In the
324 current study, TEM imaging of the PAA-CeO₂ stock solution confirmed that it is indeed the
325 number averaged results from DLS that are the most accurate in terms of size (Figure S3,
326 Supplementary Information). Here the average PAA-CeO₂ particles size ranged between 9.1
327 nm and 24.8 nm for both PAA-CeO₂ concentrations in all media types studied, which
328 corresponds more accurately to the crystallite size determined by TEM (4-10 nm).

329

330 The observed dispersion stability is in contrast to the behaviour of ‘pristine’ CeO₂ ENPs in
331 algae and other ecotoxicity media, where unstable dispersions and agglomeration are typically
332 observed (van Hoecke et al., 2009; Rogers et al., 2010; Manier et al., 2011; Rodea-Palomares
333 et al., 2011; Manier et al., 2013). Furthermore, there was no significant difference in average
334 hydrodynamic diameter (Figure 1 A-C) and zeta potential (Figure 1 D-F) between samples
335 with and without SR-NOM. Previous studies have reported that increasing concentrations of
336 humic acids and alginate (0 – 5 mg/L) give rapidly increased zeta potential and decreased
337 average hydrodynamic size of metal oxide ENPs, showing that NOM stabilises ENPs in water
338 and prevents aggregation (Loosli et al., 2013). The data in the current study indicate that the
339 stabilising effect of the PAA on the CeO₂ ENPs outweighs any additional contribution from
340 the SR-NOM (Figure 1).

341

342 The zeta potential of the PAA-CeO₂ stock solution was -25 mV (stably dispersed), whilst in
343 all media types investigated a significant decrease was immediately observed at 0 d. This
344 indicates a rapid destabilisation of the dispersion driven by the ionic concentration in the
345 different media types (although no significant aggregation was observed over 15 d; Figure 1

346 D-F). PAA-CeO₂ concentration did not influence zeta potential significantly in MHRW and
347 M7 media. However, a significant difference between PAA-CeO₂ concentrations of 0.01 and
348 1.0 mg/L was observed for TG201 media, again indicating media type significantly effects
349 dispersion stability. Both theoretical and experimental results have confirmed that zeta
350 potential is affected not only by the suspension conditions such as pH, temperature, ionic
351 strength, and even the types of ions in the suspension, but also by the particle properties such
352 as size and concentration (Tantra et al., 2010; Wang et al., 2013).

353

354 A recent study has also highlighted the significant influence that the presence of phosphate
355 can have on increasing zeta potential and stability of CeO₂ ENP dispersions at pH 7.5 (Röhder
356 et al., 2014). Furthermore, Ce³⁺ showed formation of CePO₄(s) in the presence of phosphate.
357 In the current study, the zeta potential data are generated from CeO₂ ENPs coated in PAA and
358 dispersion in a complex aquatic system containing dissolved salts (including phosphate) and
359 NOM. It is suggested that the complex interplay of varying ionic strength between the
360 different media types, the presence of phosphate in the media and the interaction of both PAA
361 and NOM at the particle surface, is influencing the stability.

362

363 *3.4. Algae ecotoxicity studies*

364 PAA-CeO₂ growth inhibition rate EC₅₀ values (0.024 mg/L) and biomass production (0.013
365 mg/L) indicate observed toxicity results from the CeO₂ ENPs with no toxic contribution from
366 the free PAA (Table 2 and Figure 2). The free PAA concentration in the PAA-CeO₂ exposure
367 solutions ranged between 0.0096-0.128 mg/L, which was significantly lower than the EC₁₀
368 and EC₅₀ growth inhibition (47.7 and 168.5 mg/L respectively) and biomass production (34.0
369 and 94.7 mg/L respectively) values of pure PAA. The data indicate that the free PAA present
370 in the PAA-CeO₂ samples did not contribute to the overall toxicity observed, and that toxicity

371 derived directly from the PAA-CeO₂ particles. In the current study, non-stabilised CeO₂ ENPs
372 were unavailable for a direct ecotoxicological comparison with the PAA-CeO₂. However,
373 EC₅₀ growth inhibition values over a CeO₂ ENP concentration range of 4.4–29.6 mg L⁻¹ have
374 previously been reported in a number of studies for the freshwater microalga *P. subcapitata*
375 (van Hoecke et al., 2009; Rogers et al., 2010; Manier et al., 2011; Rodea-Palomares et al.,
376 2011; Manier et al., 2013). These values can be used to assess the influence of PAA
377 stabilisation on the ecotoxicity of CeO₂ ENPs. The EC₅₀ growth inhibition value for PAA-
378 CeO₂ determined in the current study (0.024 mg/L) is 2-3 orders of magnitude lower than
379 literature values for pristine CeO₂ ENPs (4.4–29.6 mg L⁻¹). This indicates that the PAA-
380 stabilised CeO₂ ENPs are significantly more toxic than pristine non-stabilised forms. The
381 increased toxicity of the PAA-CeO₂ compared to both the pure PAA and pristine CeO₂ ENPs
382 indicates that there may be a synergistic effect occurring.

383

384 In these previous studies, the measured dissolved cerium (Ce³⁺/Ce⁴⁺) concentration in CeO₂
385 ENPs suspensions was low and therefore not considered to contribute significantly to the
386 observed toxicity of the CeO₂ ENPs (van Hoecke et al., 2009; Rogers et al., 2010; Rodea-
387 Palomares et al., 2011). In the current study, a non-centrifuged sample (nominally 10 mg/L)
388 was determined to have a total Ce (dissolved and particulate) concentration of 4.88 mg/L. The
389 centrifuged sample (only dissolved Ce³⁺/Ce⁴⁺) had a total Ce concentration of 0.329 mg/L,
390 indicating the dissolved Ce³⁺/Ce⁴⁺ content was approximately 6.7%. This corresponds to a
391 dissolved Ce³⁺/Ce⁴⁺ exposure concentration range of 0.5-5.6 µg/L (Table 1). This is
392 significantly below the EC₅₀ value of dissolved Ce³⁺/Ce⁴⁺ determined for *P. subcapitata*
393 (Rodea-Palomares et al., 2011), and therefore does not appear to account for the observed
394 toxicity in the PAA-CeO₂ samples. Due to the Kelvin effect, a higher solubility/dissolution
395 kinetics may be expected for CeO₂ ENPs used in this study (4-10 nm) compared to those used

396 in other studies (10-60 nm). Furthermore, it is likely that the ultracentrifugation process is not
397 100% efficient at removing CeO₂ ENPs from the sample leading to an overestimate of the
398 dissolved Ce concentration. Although the dissolved Ce concentrations are relatively low, they
399 are certainly not negligible. It would therefore be of interest in future studies to investigate the
400 ecotoxicological effects of dissolved Ce³⁺ in the presence of PAA and other common
401 stabilising agents.

402

403 In most studies with pristine CeO₂ ENPs stable dispersions in algal exposure media did not
404 form, with the ENPs undergoing different degrees of agglomeration (van Hoecke et al., 2009;
405 Rogers et al., 2010; Manier et al., 2011; Rodea-Palomares et al., 2011; Manier et al., 2013).
406 However, primary particle size was found to influence toxicity irrespective of agglomeration,
407 with smaller nominal diameters increasing growth inhibition (van Hoecke et al., 2009). The
408 CeO₂ particles used in the current study have a nominal diameter of 4-10 nm, whilst those
409 used in other studies with *P. subcapitata* are in the range 10-60 nm (van Hoecke et al., 2009;
410 Rogers et al., 2010; Manier et al., 2011; Rodea-Palomares et al., 2011; Manier et al., 2013).
411 Therefore, it is possible that the smaller diameter of the CeO₂ ENPs used in this study may be
412 contributing to the observed increase in toxicity compared to other studies. However, the
413 increased dispersion stability and lack of significant aggregation in the PAA-CeO₂ exposure
414 samples cannot be ruled out as a contributing factor to the higher toxicity observed in this
415 study compared to previous studies with pristine CeO₂ ENPs.

416

417 3.5. Biokinetics

418 In both the current study and other literature studies, it is unclear if the mechanism of toxicity
419 for CeO₂ nanoparticles to *P. subcapitata* is through uptake or by physical interaction of algal
420 cells with the particles. No evidence of algal flocculation in the presence of PAA-CeO₂ was

421 observed during the current study. HR-ICP-MS analysis of the total Ce concentration
422 (dissolved and particulate) in the exposure media before and after removal of the algae
423 suggest that during the 72 h exposure up to 38% of the total Ce becomes directly associated
424 with the algal cells (Figure 3). However, it is unclear whether this association is direct uptake
425 or adsorption of the PAA-CeO₂ onto the surface of the algal cells. In their study, Rodea-
426 Palomares et al. (Rodea-Palomares et al., 2011) found no evidence of CeO₂ ENP uptake by
427 cells, but that their toxic mode of action appeared to require direct contact between ENPs and
428 cells. The authors suggest that cell damage most probably took place by cell wall and
429 membrane disruption, possibly due to the oxidative activity of ceria. CeO₂ ENPs have been
430 shown to induce flocculation and a clustering of particles on the cell surface of *P. subcapitata*,
431 whereby the interaction of CeO₂ ENP with the cell surface also lead to an increase of cell
432 membrane permeability (van Hoecke et al., 2009; Rodea-Palomares et al., 2011). However,
433 when Röhder et al. (Röhder et al., 2014) compared a cell wall free mutant and a wild strain of
434 the freshwater alga *Chlamydomonas reinhardtii* they concluded that cell wall plays a minor
435 role on the toxicity to CeO₂ ENPs. Furthermore, a flocculation of cells was observed
436 following exposure to agglomerated CeO₂ ENPs, and may represent a general response to
437 various stresses (Rakesh et al., 2014), although whether this process impairs growth through
438 shading or by limiting the diffusion of nutrients remains to be evaluated (Röhder et al., 2014).

439

440 Algal cells collected from the ecotoxicity experiments were analysed by TOF-SIMS in order
441 to investigate their interaction with the PAA-CeO₂. Specific alterations in the cell membrane
442 composition (see Figure 5) of *P. subcapitata* could be used to separate unexposed control
443 cells at 0 h from unexposed control cells harvested after 72 h, and from PAA-CeO₂ exposed
444 cells at 0 h and 72 h, using algal cell wall biomarker compounds (see Figure 4). Generally
445 three membrane alterations can be identified (Figure 5 A-C). The first is an increase in certain

446 biomarker compounds directly after PAA-CeO₂ exposure (0 h) in comparison to unexposed
447 controls at both 0 h and 72h, indicating a direct response to the presence of the PAA-CeO₂
448 (Figure 5A). In particular, the acquired surface spectra of PAA-CeO₂ exposed algae at 0 h and
449 72h exposure showed a significant increase in ion m/e 327 (Yang et al., 2013), which is
450 tentatively assigned to a hydroxy eicosanoic acid. This hydroxy fatty acid is commonly found
451 in algae and micro algae (Blokker et al., 1998; Sasso et al., 2012), and in this study already
452 exhibited a significant increase at 0 h in PAA-CeO₂ exposed cells. Oxidised fatty acids are
453 known to be protective against oxidative stress and may even serve as signalling molecules
454 for inter-individual as well as inter-species communication (Pohl et al., 2014). A similar
455 behaviour is observed for ions m/e 504, m/e 846 and m/e 1600. Ion m/e 504 is tentatively
456 assigned to a lyso phosphatidyl ethanolamine (lyso PE C20:2). Lyso phosphatidyl
457 ethanolamines have already been identified in micro algae (He et al., 2011) and higher
458 amounts of lyso phosphatidyl ethanolamines are associated with the inhibition of
459 phospholipase D which causes enhanced cell wall lipid degradation and oxidative stress
460 (Munnik, 2001; Peters et al., 2007). Ion m/e 846 was tentatively assigned to a triacylglyceride
461 (TG C52:8). An increase in triacylglyceride levels was also observed in micro algae under
462 environmental stress and especially as a result of heavy metal exposure (Sharma et al., 2012).
463 Ion m/e 1600 could not be assigned to any known compound. These results are consistent
464 with reports describing the generation of reactive oxygen species (ROS) from CeO₂ ENPs
465 which are involved in CeO₂ ENP toxicity to mammalian cells (Auffan et al., 2009b). In
466 contrast, other studies have reported CeO₂ ENPs exhibit a scavenging ability and can reduce
467 oxidative stress (Amin et al., 2011). The contradictory ability of CeO₂ ENPs to both generate
468 and scavenge ROS seems to depend on the redox state, which can change between Ce(III) and
469 Ce(IV) (Auffan et al., 2009a). In the current study, PAA-CeO₂ appears to generate ROS
470 which elicit a response from the algal cells and maybe also be contributing to the observed

471 acute toxicity (growth inhibition). However, we are unable to conclude whether this
472 represents high ROS formation compared to other CeO₂ ENPs studied and therefore
473 contributing to the increased toxicity of the PAA-CeO₂. Furthermore, it is possible that the
474 physicochemical properties of the CeO₂ ENPs and/or the presence of PAA is resulting in the
475 increased formation of ROS which, in turn, may increase the observed toxicity.

476
477 A second alteration could be observed, where the control sample at 0 h had high levels of
478 certain biomarker compounds, which were observed to be significantly decreased in 72 h
479 controls and in both 0 h and 72 h PAA-CeO₂ exposed cells (Figure 5B). Control and PAA-
480 CeO₂ exposed cells at 72 h exhibited slightly lower levels than PAA-CeO₂ exposed cells at 0
481 h. Ions m/e 341 and m/e 343 could be tentatively assigned to caffeic acid-O-glycoside and
482 homovanillic acid-O-glycoside respectively. Micro algae have the capability to synthesize
483 caffeic acid from the amino acid phenylalanine (El-Baky et al., 2009). This study also showed
484 that caffeic acid exhibited antioxidant effects on CCl₄-induced lipid peroxidation and could
485 serve as a radical scavenger in micro algae. The decrease in caffeic acid biosynthesis in the
486 present study may indicate an age related loss of lipid peroxidation recovery and radical
487 scavenging activity, which could be triggered already at time 0h in PAA-CeO₂ exposed cells.
488 Ions m/e 895 and m/e 897, tentatively assigned to phosphatidylinositols (PI(O-C40:6) and
489 PI(O-C40:5)) showed a similar mechanism.

490
491 A third biomarker alteration exhibited highest levels in both the unexposed and the exposed
492 control cells at time point 0 h. Over the 72 h duration of the test, a significant decrease in the
493 concentration of these compounds was observed in both sample types (Figure 5C). A number
494 of previous studies have also reported a rapid change (e.g. within 5 mins) in the state of the
495 cell membrane following exposure to oxidative stress causing chemicals (Alvarez-Ordóñez et

496 al., 2010; Hale et al., 2011). This mechanism always seems to be associated with a subsequent
497 secondary change of the cell membrane, typically observed after 1 to 3 days. For the first
498 time, the current study indicates specific biomarker compounds related to these mechanisms.
499 The concentration of ions m/e 330 and m/e 332, tentatively assigned to sialic acid and
500 dehydrosialic acid decreased in samples (both control and PAA-CeO₂ exposed) from 0 h to 72
501 h in a similar way. This indicates a general metabolic mechanism, unrelated PAA-CeO₂
502 exposure, is occurring in *P. subcapitata* cultures over time. Sialic acid probably arises from
503 terminally sialylated N-linked oligosaccharides, which were already identified in green algae
504 (Mamedov et al., 2011). Sialic acid decrease has already been characterized as a biomarker
505 for muscle aging in mice and may also represent a biomarker for aging effects in *P.*
506 *subcapitata* (Hanisch et al., 2013). The data show that this response in the algae is time
507 dependent and not dependent upon PAA-CeO₂ exposure, representing basic age related
508 metabolomic and lipidomic changes under conditions applied in the present study.

509

510

511 **4. Conclusions**

512 Under typical environmental conditions it is likely that PAA-stabilised CeO₂ ENPs will not
513 undergo significant agglomeration and settle out of the aqueous phase. The use of stabilising
514 agents in the synthesis of ENPs to provide useful physicochemical properties for technology
515 applications may therefore lead to significant differences in the environmental behaviour
516 compared to pristine ENP analogues. Stably dispersed PAA-CeO₂ appear to elicit a
517 toxicological response in *P. subcapitata* at lower concentrations than pristine CeO₂ ENPs
518 which rapidly agglomerate. Despite this, the PAA-CeO₂ concentrations needed to cause short-
519 term effects appear to be much higher in comparison to the background cerium concentration
520 in natural waters (Röhder et al., 2014). However, release of PAA-CeO₂ would offer the

521 possibility of increasing environmental concentrations of stably dispersed nanoparticle ceria
522 in natural waters. Owing to the low dissolution rate of $\text{Ce}^{3+}/\text{Ce}^{4+}$, PAA-CeO₂ may have a
523 considerable residence time in natural waters. As the modification of ENP surface chemistry
524 and the use of stabilising agents is becoming more common in the synthesis of ENPs for
525 technology applications, there is a need to generate new ecotoxicity data in addition to that
526 available for ‘pristine’ materials.

527

528 **Acknowledgements**

529 The work reported here has been undertaken as part of the AERTO project ‘Value from
530 Waste’, the EU FP7 project ‘NANoREG’ (Grant Agreement number 310584) and the
531 Research Council of Norway project ‘NanoSorb’ (Grant Agreement number 209685/E50).
532 The authors wish to thank these projects for their financial support. The authors acknowledge
533 the essential technical assistance of Kristin Bonaunet, Lisbet Støen, Inger Steinsvik, Anne
534 Rein Hatleveit, Calin Marioara (SINTEF Materials and Chemistry), Galina Alvarez (SP) and
535 Syverin Lierhagen (NTNU).

536

537 **References**

- 538 Adegboyega NF, Sharma VK, Siskova K, Zbořil R, Sohn M, Schultz BJ, Banerjee S. Interactions
539 of Aqueous Ag⁺ with Fulvic Acids: Mechanisms of Silver Nanoparticle Formation and
540 Investigation of Stability. *Environmental Science & Technology* 2012; 47: 757-764.
- 541 Alvarez-Ordóñez A, Prieto M. Changes in Ultrastructure and Fourier Transform Infrared
542 Spectrum of *Salmonella enterica* Serovar Typhimurium Cells after Exposure to Stress
543 Conditions. *Applied and Environmental Microbiology* 2010; 76: 7598-7607.
- 544 Amin KA, Hassan MS, Awad el ST, Hashem KS. The protective effects of cerium oxide
545 nanoparticles against hepatic oxidative damage induced by monocrotaline. *Int J*
546 *Nanomedicine* 2011; 6: 143-149.
- 547 Auffan M, Rose J, Wiesner MR, Bottero J-Y. Chemical stability of metallic nanoparticles: A
548 parameter controlling their potential cellular toxicity in vitro. *Environmental Pollution*
549 2009a; 157: 1127-1133.
- 550 Auffan M, Rose J, Orsiere T, De Meo M, Thill A, Zeyons O, Proux O, Masion A, Chaurand P,
551 Spalla O, Botta A, Wiesner MR, Bottero J-Y. CeO₂ nanoparticles induce DNA damage
552 towards human dermal fibroblasts in vitro. *Nanotoxicology* 2009b; 3: 161-171.
- 553 Baalousha M, Nur Y, Römer I, Tejamaya M, Lead JR. Effect of monovalent and divalent
554 cations, anions and fulvic acid on aggregation of citrate-coated silver nanoparticles.
555 *Science of the Total Environment* 2013; 454-455: 119-131.
- 556 Blokker P, Schouten S, van den Ende H, De Leeuw JW, Sinninghe Damsté JS. Cell wall-specific
557 ω-hydroxy fatty acids in some freshwater green microalgae. *Phytochemistry* 1998;
558 49: 691-695.
- 559 Booth A, Justynska J, Kubowicz S, Johnsen H, Frenzel M. Influence of salinity, dissolved
560 organic carbon and particle chemistry on the aggregation behaviour of methacrylate-
561 based polymeric nanoparticles in aqueous environments. *International Journal of*
562 *Environment and Pollution* 2013; 52: 15 - 31.
- 563 Chane-Ching JY. Alkali metal and ammonium hydroxy nitrates with cerium. In: Google
564 Patents, 1994.
- 565 El-Baky HHA, El Baz FK, El-Baroty GS. Production of phenolic compounds from *Spirulina*
566 *maxima* microalgae and its protective effects. *African Journal of Biotechnology* 2009;
567 8: 7059-7067.
- 568 Gallego-Urrea JA, Perez Holmberg J, Hasselov M. Influence of different types of natural
569 organic matter on titania nanoparticle stability: effects of counter ion concentration
570 and pH. *Environmental Science: Nano* 2014; 1: 181-189.
- 571 García A, Espinosa R, Delgado L, Casals E, González E, Puentes V, Barata C, Font X, Sánchez A.
572 Acute toxicity of cerium oxide, titanium oxide and iron oxide nanoparticles using
573 standardized tests. *Desalination* 2011; 269: 136-141.
- 574 Haase A, Arlinghaus HF, Tentschert J, Jungnickel H, Graf P, Manton A, Draude F, Galla S,
575 Plendl J, Goetz ME, Masic A, Meier W, Thünemann AF, Taubert A, Luch A. Application
576 of Laser Postionization Secondary Neutral Mass Spectrometry/Time-of-Flight
577 Secondary Ion Mass Spectrometry in Nanotoxicology: Visualization of Nanosilver in
578 Human Macrophages and Cellular Responses. *ACS Nano* 2011; 5: 3059-3068.
- 579 Hale John P, Winlove CP, Petrov Peter G. Effect of Hydroperoxides on Red Blood Cell
580 Membrane Mechanical Properties. *Biophysical Journal* 2011; 101: 1921-1929.

581 Hanisch F, Weidemann W, Großmann M, Joshi PR, Holzhausen H-J, Stoltenburg G, Weis J,
582 Zierz S, Horstkorte R. Sialylation and Muscle Performance: Sialic Acid Is a Marker of
583 Muscle Ageing. *PLoS one* 2013; 8: e80520.

584 He H, Rodgers RP, Marshall AG, Hsu CS. Algae Polar Lipids Characterized by Online Liquid
585 Chromatography Coupled with Hybrid Linear Quadrupole Ion Trap/Fourier Transform
586 Ion Cyclotron Resonance Mass Spectrometry. *Energy & Fuels* 2011; 25: 4770-4775.

587 Johnston BD, Scown TM, Moger J, Cumberland SA, Baalousha M, Linge K, van Aerle R, Jarvis
588 K, Lead JR, Tyler CR. Bioavailability of Nanoscale Metal Oxides TiO₂, CeO₂, and ZnO to
589 Fish. *Environmental Science & Technology* 2010; 44: 1144-1151.

590 Jungnickel H, Jones EA, Lockyer NP, Oliver SG, Stephens GM, Vickerman JC. Application of
591 TOF-SIMS with Chemometrics To Discriminate between Four Different Yeast Strains
592 from the Species *Candida glabrata* and *Saccharomyces cerevisiae*. *Analytical
593 Chemistry* 2005; 77: 1740-1745.

594 Karakoti AS, Monteiro-Riviere NA, Aggarwal R, Davis JP, Narayan RJ, Self WT, McGinnis J, Seal
595 S. Nanoceria as antioxidant: Synthesis and biomedical applications. *JOM* 2008; 60: 33-
596 37.

597 Keller AA, Wang H, Zhou D, Lenihan HS, Cherr G, Cardinale BJ, Miller R, Ji Z. Stability and
598 Aggregation of Metal Oxide Nanoparticles in Natural Aqueous Matrices.
599 *Environmental Science & Technology* 2010; 44: 1962-1967.

600 Loosli F, Le Coustumer P, Stoll S. TiO₂ nanoparticles aggregation and disaggregation in
601 presence of alginate and Suwannee River humic acids. pH and concentration effects
602 on nanoparticle stability. *Water Research* 2013; 47: 6052-6063.

603 Louie SM, Tilton RD, Lowry GV. Effects of Molecular Weight Distribution and Chemical
604 Properties of Natural Organic Matter on Gold Nanoparticle Aggregation.
605 *Environmental Science & Technology* 2013; 47: 4245-4254.

606 Mamedov T, Yusibov V. Green algae *Chlamydomonas reinhardtii* possess endogenous
607 sialylated N-glycans. *FEBS Open Bio* 2011; 1: 15-22.

608 Manier N, Garaud M, Delalain P, Aguerre-Chariol O, Pandard P. Behaviour of ceria
609 nanoparticles in standardized test media – influence on the results of
610 ecotoxicological tests. *Journal of Physics: Conference Series* 2011; 304: 012058.

611 Manier N, Bado-Nilles A, Delalain P, Aguerre-Chariol O, Pandard P. Ecotoxicity of non-aged
612 and aged CeO₂ nanomaterials towards freshwater microalgae. *Environmental
613 Pollution* 2013; 180: 63-70.

614 Munnik T. Phosphatidic acid: an emerging plant lipid second messenger. *Trends Plant Sci*
615 2001; 6: 227-233.

616 OECD. Freshwater Alga and Cyanobacteria, Growth Inhibition Test. Proposal for updating
617 Guideline 201. Organisation for Economic Cooperation and Development (OECD),
618 Paris. 2002, 21.

619 OECD. Freshwater Alga and Cyanobacteria, Growth Inhibition Test. . Organisation for
620 Economic Cooperation and Development (OECD), Paris. 2011, 25.

621 Park B, Martin P, Harris C, Guest R, Whittingham A, Jenkinson P, Handley J. Initial in vitro
622 screening approach to investigate the potential health and environmental hazards of
623 EnviroxTM - a nanoparticulate cerium oxide diesel fuel additive. *Particle and Fibre
624 Toxicology* 2007; 4: 12.

625 Peters NT, Logan KO, Miller AC, Kropf DL. Phospholipase D signaling regulates microtubule
626 organization in the furoid alga *Silvetia compressa*. *Plant Cell Physiol* 2007; 48: 1764-
627 1774.

628 Pohl C, Kock J. Oxidized Fatty Acids as Inter-Kingdom Signaling Molecules. *Molecules* 2014;
629 19: 1273-1285.

630 Quik JTK, Stuart MC, Wouterse M, Peijnenburg W, Hendriks AJ, van de Meent D. Natural
631 colloids are the dominant factor in the sedimentation of nanoparticles.
632 *Environmental Toxicology and Chemistry* 2012; 31: 1019-1022.

633 Quik JTK, Lynch I, Hoecke KV, Miermans CJH, Schamphelaere KACD, Janssen CR, Dawson KA,
634 Stuart MAC, Meent DVD. Effect of natural organic matter on cerium dioxide
635 nanoparticles settling in model fresh water. *Chemosphere* 2010; 81: 711-715.

636 Rakesh S, Saxena S, Dhar D, Prasanna R, Saxena A. Comparative evaluation of inorganic and
637 organic amendments for their flocculation efficiency of selected microalgae. *J Appl*
638 *Phycol* 2014; 26: 399-406.

639 Rodea-Palomares I, Boltes K, Fernández-Piñas F, Leganés F, García-Calvo E, Santiago J, Rosal
640 R. Physicochemical Characterization and Ecotoxicological Assessment of CeO₂
641 Nanoparticles Using Two Aquatic Microorganisms. *Toxicological Sciences* 2011; 119:
642 135-145.

643 Rodea-Palomares I, Gonzalo S, Santiago-Morales J, Leganés F, García-Calvo E, Rosal R,
644 Fernández-Piñas F. An insight into the mechanisms of nanoceria toxicity in aquatic
645 photosynthetic organisms. *Aquatic Toxicology* 2012; 122–123: 133-143.

646 Rogers NJ, Franklin NM, Apte SC, Batley GE, Angel BM, Lead JR, Baalousha M. Physico-
647 chemical behaviour and algal toxicity of nanoparticulate CeO₂ in freshwater.
648 *Environmental Chemistry* 2010; 7: 50-60.

649 Röhder LA, Brandt T, Sigg L, Behra R. Influence of agglomeration of cerium oxide
650 nanoparticles and speciation of cerium(III) on short term effects to the green algae
651 *Chlamydomonas reinhardtii*. *Aquatic Toxicology* 2014; 152: 121-130.

652 Salazar-Sandoval EJ, Johansson MKG, Ahniyaz A. Aminopolycarboxylic acids as a versatile
653 tool to stabilize ceria nanoparticles - a fundamental model experimentally
654 demonstrated. *RSC Advances* 2014; 4: 9048-9055.

655 Sánchez A, Recillas S, Font X, Casals E, González E, Puentes V. Ecotoxicity of, and remediation
656 with, engineered inorganic nanoparticles in the environment. *TrAC Trends in*
657 *Analytical Chemistry* 2011; 30: 507-516.

658 Sasso S, Pohnert G, Lohr M, Mittag M, Hertweck C. Microalgae in the postgenomic era: a
659 blooming reservoir for new natural products. *FEMS Microbiology Reviews* 2012; 36:
660 761-785.

661 Sehgal A, Lalatonne Y, Berret JF, Morvan M. Precipitation–Redispersion of Cerium Oxide
662 Nanoparticles with Poly(acrylic acid): Toward Stable Dispersions. *Langmuir* 2005; 21:
663 9359-9364.

664 Sharma KK, Schuhmann H, Schenk PM. High Lipid Induction in Microalgae for Biodiesel
665 Production. *Energies* 2012; 5: 1532-1553.

666 Tantra R, Schulze P, Quincey P. Effect of nanoparticle concentration on zeta-potential
667 measurement results and reproducibility. *Particuology* 2010; 8: 279-285.

668 Tentschert J, Draude F, Jungnickel H, Haase A, Manton A, Galla S, Thünemann AF, Taubert A,
669 Luch A, Arlinghaus HF. TOF-SIMS analysis of cell membrane changes in functional

670 impaired human macrophages upon nanosilver treatment. *Surface and Interface*
671 *Analysis* 2013; 45: 483-485.

672 Thompson CE, Jungnickel H, Lockyer NP, Stephens GM, Vickerman JC. ToF-SIMS studies as a
673 tool to discriminate between spores and vegetative cells of bacteria. *Applied Surface*
674 *Science* 2004; 231–232: 420-423.

675 US EPA. *Methods for Measuring the Acute Toxicity of Effluents and Receiving Waters to*
676 *Freshwater and Marine Organisms*. EPA-821-R-02-012. U.S. Environmental Protection
677 Agency, Washington, DC. 2002, 31-33.

678 van Hoecke K, De Schampelaere KAC, Van der Meeren P, Smagghe G, Janssen CR.
679 Aggregation and ecotoxicity of CeO₂ nanoparticles in synthetic and natural waters
680 with variable pH, organic matter concentration and ionic strength. *Environmental*
681 *Pollution* 2011; 159: 970-976.

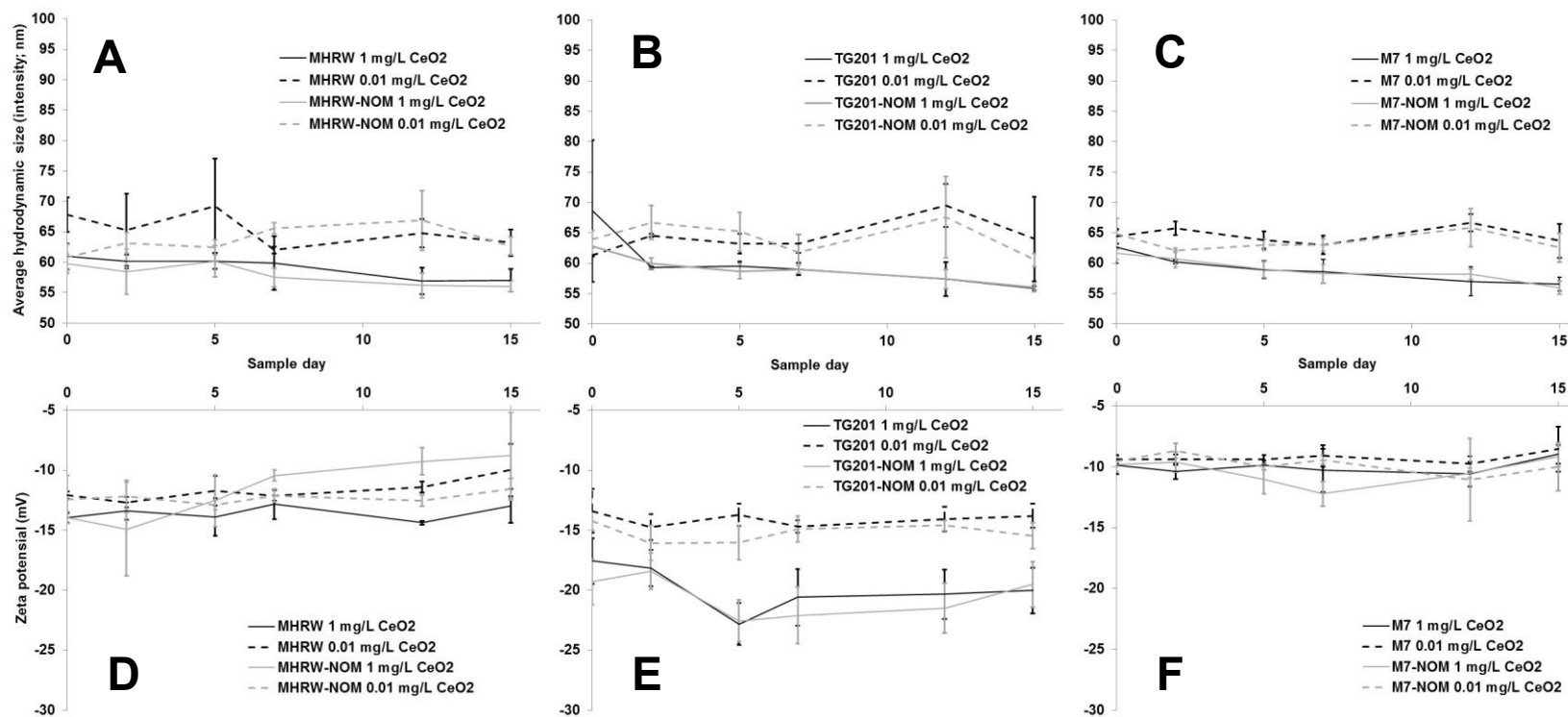
682 van Hoecke K, Quik JTK, Mankiewicz-Boczek J, de Schampelaere KAC, Elsaesser A, van der
683 Meeren P, Barnes C, McKerr G, Howard CV, van de Meent D, Rydzyński K, Dawson KA,
684 Salvati A, Lesniak A, Lynch I, Silversmit G, de Samber B, Vincze L, Janssen CR. Fate and
685 Effects of CeO₂ Nanoparticles in Aquatic Ecotoxicity Tests. *Environmental Science &*
686 *Technology* 2009; 43: 4537-4546.

687 Wang H, Keller AA, Clark KK. Natural organic matter removal by adsorption onto magnetic
688 permanently confined micelle arrays. *Journal of Hazardous Materials* 2011; 194: 156-
689 161.

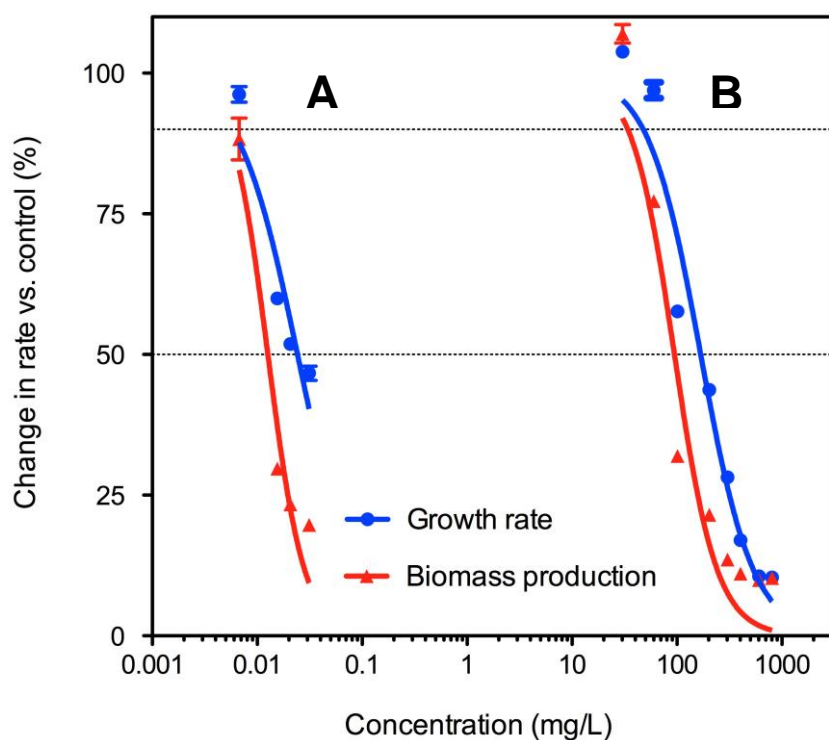
690 Wang N, Hsu C, Zhu L, Tseng S, Hsu J-P. Influence of metal oxide nanoparticles concentration
691 on their zeta potential. *Journal of Colloid and Interface Science* 2013; 407: 22-28.

692 Xu C, Qu X. Cerium oxide nanoparticle: a remarkably versatile rare earth nanomaterial for
693 biological applications. *NPG Asia Mater* 2014; 6: e90.

694 Yang N-Y, Yang Y-F, Li K. Analysis of Hydroxy Fatty Acids from the Pollen of *Brassica*
695 *campestris* L. var. *oleifera* DC. by UPLC-MS/MS. *Journal of Pharmaceutics* 2013; 2013:
696 6.
697
698

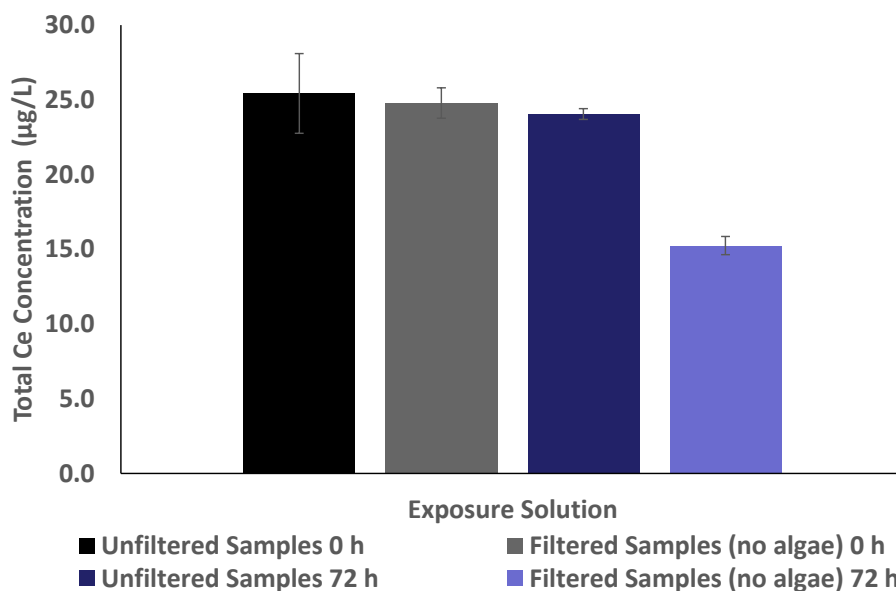


702 *Figure 1. Hydrodynamic size (nm) in A) MHRW, B) TG201 and C) M7 media and zeta potential (mV) measurements in D) MHRW, E) TG201*
703 *and F) M7 media during 15 day stability studies at two different suspension concentrations of PAA-CeO₂ (0.01 and 1.0 mg/L). Hydrodynamic*
704 *size is displayed as intensity averaged sizes. Error bars represent standard deviation (n=3).*



705

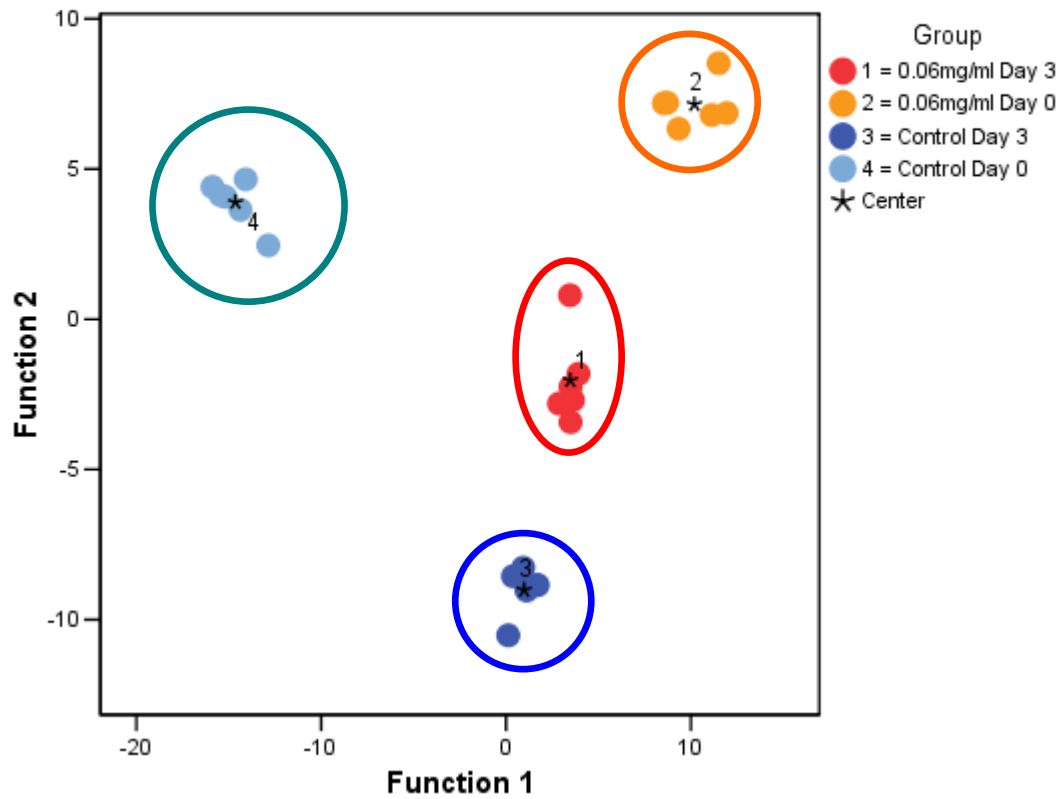
706 *Figure 2. Change in growth rate and biomass production as a function of A) PAA-CeO₂ and*
 707 *B) pure PAA. Both data sets are plotted according to the CeO₂ exposure concentrations*
 708 *determined using HR-ICP-MS.*
 709



710

711 *Figure 3. Total Ce concentration (µg/L) in filtered samples (no algae) and unfiltered samples*
 712 *(containing algae) collected at 0 h and 72 h. Error bars represent standard deviation (n=3).*
 713

Fisher's Discriminant Function



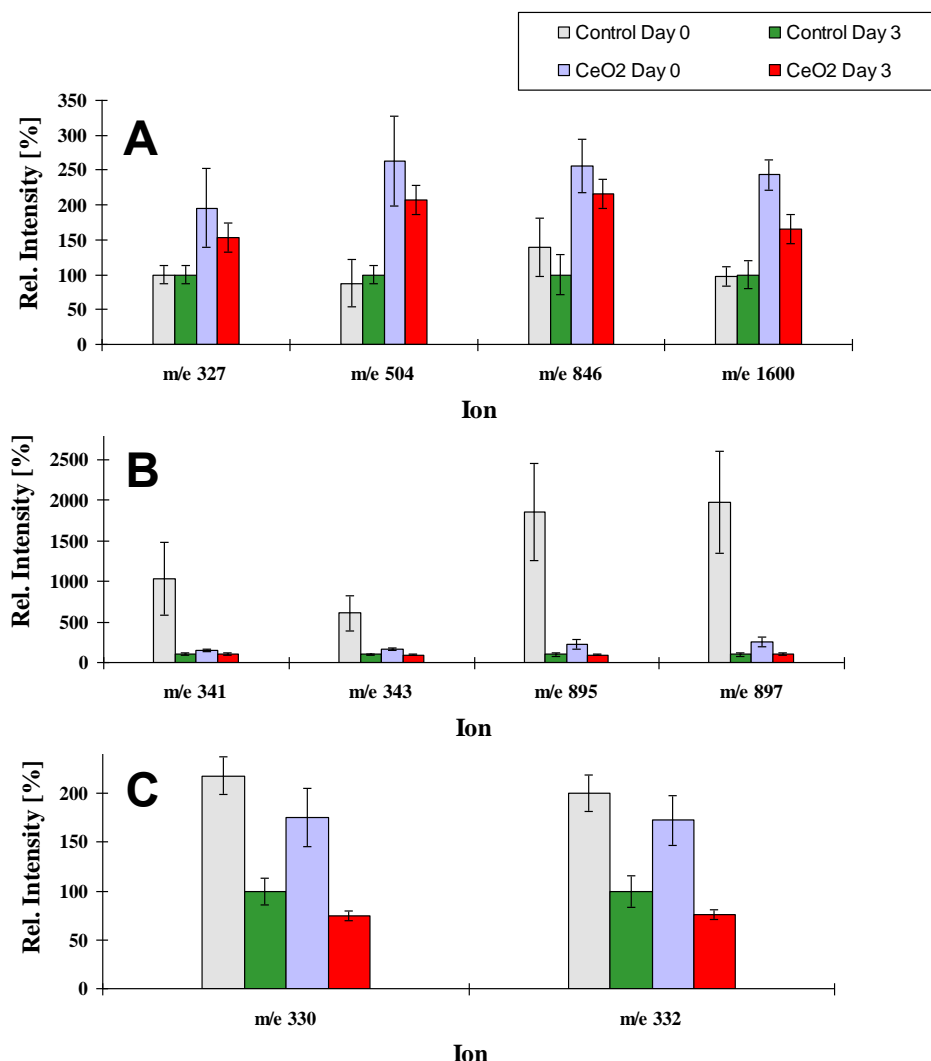
714

715

716 *Figure 4. TOF-SIMS analysis changes in compound composition of the cell wall of*
717 *Pseudokirchneriella subcapitata* *after nanoparticle treatment. The diagram shows the values*
718 *of the discriminant scores obtained from Fisher's discriminant analysis of 24 algal samples*
719 *for all ions, which were selected to discriminate between untreated micro algae cultures at*
720 *day 0 and day 3 and micro algae, treated with 0.06mg/ml CeO₂ at day 0 and day 3.*

721

722



723
724
725
726
727
728
729
730
731
732
733
734
735

Figure 5. Histogram comparisons of ion yields for characteristic biomarker ions which were used to separate the four treatment groups. The biomarker ions indicate three different biomarker alterations: A) where compounds loaded high on function 1 (>0.9; Figure 4) and showed significantly higher levels in exposed samples at day 0 and day 3 in comparison to control samples. B) where compounds loaded high (>0.9; Figure 4) on function 1 or function 2 and showed significantly higher levels in control samples at day 0 compared to controls at day 3 and exposed cells at day 0 and day 3. C) where compounds loaded high (>0.9; Figure 4) on function 1 or function 2 and showed significantly higher levels in control and exposed samples at day 0 compared to control and exposed samples at day 3. For the relative intensity, the mean of the control group at 72 h was taken as 100% in all cases.

736 **Tables**

737 *Table 1. Summary of the nominal PAA-CeO₂ concentrations, total Ce concentration at 0 h*
 738 *and 72 h, the calculated dissolved Ce concentration at 0 h and the free PAA concentration at*
 739 *0 h in each of the exposure samples used in growth inhibition tests with P. subcapitata.*

Nominal PAA-CeO ₂ exposure concentration (µg/L)	Total Ce concentration (µg/L)				Dissolved Ce concentration at 0 h (µg/L)	Free PAA concentration at 0 h (µg/L)
	0 h	%rsd	72 h	%rsd		
15	5.5	2.8	6.5	2	0.5	9.6
25	12.6	8.8	10.2	1.5	1.0	16
40	16.8	4.4	15.3	1.8	1.4	25.6
60	25.4	10.5	24.0	1.5	2.1	38.4
100	32.7	9.5	52.4	4.4	2.7	64
200	67.5	12	81.0	4.5	5.6	128

740

741

742

743 *Table 2. Calculated effect concentrations of pure PAA and PAA stabilised CeO₂*
 744 *nanoparticles (PAA-CeO₂) to the freshwater algae, Pseudokirchneriella subcapitata, in a 72 h*
 745 *growth inhibition test.*

	EC ₁₀ mg/L (95% CI)		EC ₅₀ mg/L (95% CI)	
	<i>Growth Rate</i>	<i>Biomass production</i>	<i>Growth Rate</i>	<i>Biomass production</i>
PAA	47.7 (36.2 - 63.1)	34.0 (24.3 - 47.6)	168.5 (149.3 - 190.1)	94.7 (81.3 - 110.3)
PAA-CeO ₂	0.0058 (0.0036 - 0.0094)	0.0053 (0.0037 - 0.0074)	0.024 (0.021 - 0.028)	0.013 (0.011 - 0.015)

746